

Soil sealing vulnerability in high-value agricultural land: A multicriteria GIS-based approach

Vulnerabilidad al sellamiento en suelos
agrícolas de alto valor: un enfoque SIG multicriterio

Andrés Fernando Echeverri-Sánchez¹; Robin Alexis Olaya²; María del Mar Carreño-Sánchez³;
Clever Gustavo Becerra-Romero⁴; Jhony Armando Benavides-Bolaños⁵

¹. Universidad del Valle, Cali, Colombia, andres.echeverri@correounivalle.edu.co, <https://orcid.org/0000-0002-8477-9773>

². Universidad del Valle, Cali, Colombia, robin.olaya@correounivalle.edu.co, <https://orcid.org/0000-0001-7956-3612>

³. Universidad del Valle, Cali, Colombia, maria.delmar.carreno@correounivalle.edu.co,
<https://orcid.org/0009-0000-3387-6891>

⁴. Corporación Autónoma Regional del Valle del Cauca, Cali, Colombia, clever-gustavo.becerra@cvc.gov.co,
<https://orcid.org/0000-0003-0894-7859>

⁵. Universidad del Valle, Cali, Colombia, jhony.benavides@correounivalle.edu.co,
<https://orcid.org/0000-0001-9252-3770> (Correspondence)

Cite: Echeverri-Sánchez, A. F.; Olaya, R. A.; Carreño-Sánchez, M. M.; Becerra-Romero, C. G.; Benavides-Bolaños, J. A. (2025). Soil sealing vulnerability in high-value agricultural land: A multicriteria GIS-based approach. *Revista de Ciencias Agrícolas*. 42(3): e3277. <https://doi.org/10.22267/rcia.20254203.277>

ABSTRACT

Soil sealing remains an under-addressed threat to agricultural sustainability, particularly in rapidly urbanizing rural-urban interfaces. To address this challenge, a spatially explicit Soil Sealing Vulnerability Index (SSVI) was developed for 126,734.87 hectares of agricultural land in the Guachal and Amaime watersheds (GAWs), Valle del Cauca, Colombia. The SSVI integrates seven spatially referenced biophysical and institutional parameters—terrain slope, parcel size, road proximity, proximity to surface water bodies, agrological soil class, urban growth trends (2000–2024), and municipal land-use designations—using a multi-criteria analysis structured by expert consensus through the Analytic Hierarchy Process. With strong internal consistency, demonstrated by a Consistency Ratio (CR) of 2.51% that confirms the logical stability of expert judgments, the SSVI provides spatial support for decision-making in municipal land-use planning. Independent validation is deferred until sealing datasets become available, using a replicable concordance workflow. Results indicate that 42.54% of the GAWs area presents moderate vulnerability, 19.01% low vulnerability, 1.00% (1,270.1 ha) high vulnerability, and 37.44% corresponds to exclusion zones (e.g., urban cores and protected areas). Importantly, 938.7 ha of environmentally restricted soils and 228.8 ha of Mollisols fall within high-vulnerability zones, highlighting the model's ability to identify policy-relevant risks. This study introduces the first spatially resolved SSVI tailored to Colombia's regulatory landscape, demonstrating that vulnerability is more strongly influenced by institutional planning than by natural land constraints. Although technically replicable, effective application requires high-resolution spatial datasets and local expert participation. Integration into municipal planning instruments is essential to translate technical findings into policy action.

Keywords: decision support systems; environmental impact; land cover change; land use planning; peri-urban areas; soil properties.

RESUMEN

El sellado del suelo sigue siendo una amenaza subestimada para la sostenibilidad agrícola, particularmente en las interfaces rurales-urbanas sometidas a urbanización acelerada. Para abordar este desafío, se desarrolló un Índice de Vulnerabilidad al Sellado del Suelo (IVSS)

espacialmente explícito para 126.734,87 hectáreas agrícolas en las cuencas de los ríos Guachal y Amaime (CRGA), Valle del Cauca, Colombia. El IVSS integra siete parámetros biofísicos e institucionales georreferenciados: pendiente, tamaño de parcela, cercanía a vías y cuerpos de agua superficial, clase agrológica, crecimiento urbano (2000–2024) y designaciones municipales de uso del suelo, mediante un análisis multicriterio estructurado con el Proceso de Jerarquía Analítica y consenso experto. Con una fuerte consistencia interna, demostrada por un Índice de Consistencia (IC) del 2,51% que confirma la estabilidad lógica de los juicios de los expertos, el IVSS proporciona apoyo espacial para la toma de decisiones en la planificación municipal del uso del suelo. La validación independiente se pospone hasta que existan conjuntos de datos de sellamiento disponibles, utilizando un flujo de trabajo de concordancia replicable. Se identificó que el 42,54% del área presenta vulnerabilidad moderada, el 19,01% baja, el 1,00% (1.270,1 ha) alta, y el 37,44% corresponde a zonas de exclusión (e.g., núcleos urbanos y áreas protegidas). Destacan 938,7 ha de suelos ambientalmente restringidos y 228,8 ha de Mollisoles en zonas de alta vulnerabilidad, evidenciando la capacidad del modelo para identificar riesgos relevantes en política pública. Este es el primer IVSS adaptado al marco regulatorio colombiano, y demuestra que la vulnerabilidad está más influenciada por la planificación institucional que por limitantes naturales del suelo. Su implementación requiere datos espaciales detallados y participación experta local para incidir eficazmente en la planificación territorial.

Palabras clave: áreas periurbanas; cambio de cobertura del suelo; impacto ambiental; planificación del uso del suelo; propiedades del suelo; sistemas de apoyo a la toma de decisiones.

INTRODUCTION

Soil sealing, defined as the permanent or semi-permanent coverage of land with impermeable materials such as asphalt or concrete, is among the most pressing environmental challenges of the 21st century. Closely tied to global urbanization and infrastructure expansion, this phenomenon fundamentally alters the structure and functionality of soils, impairing their capacity to provide essential ecosystem services such as water regulation, carbon sequestration, nutrient cycling, and biodiversity support (Dadi *et al.*, 2022). The loss of these services, particularly in peri-urban areas, undermines environmental sustainability and food security while exacerbating socio-economic vulnerabilities across rural and urban interfaces (Garschagen & Romero-Lankao, 2015; Yu *et al.*, 2019; Ziem Bonye *et al.*, 2021).

The physical and biogeochemical consequences of soil sealing are both severe and quantifiable. Sealed soils experience structural degradation, with increased bulk density (e.g., up to 1.32 g/cm³ vs. 0.86 g/cm³ in unsealed areas), reduced porosity, and diminished infiltration capacity—especially in silty soils, where final infiltration rates may drop by over 50% under moderate rainfall (Assouline & Mualem, 2002; O’Riordan *et al.*, 2021). Crust formation also intensifies, particularly in smectitic clays (17.77 mm vs. 3.84 mm in kaolinitic soils) (Mrubata *et al.*, 2024). These changes are paralleled by reduced microbial activity (e.g., lower C/N ratios), impaired N retention, and diminished C sequestration and moisture-holding capacity (Wei *et al.*, 2014; Tóth *et al.*, 2022). In Functional Urban Areas across Europe, over 4 million tons of carbon and 670 million m³ of water storage capacity were lost between 2012 and 2018 due to progressive sealing (Tóth *et al.*, 2022).

Case studies from diverse geographic contexts confirm these impacts. In Mediterranean landscapes, soil sealing contributes to agroecological fragmentation, while in Chinese cities like Yixing and Hangzhou Bay, rapid urban expansion has altered soil morphology and connectivity (Xiao *et al.*, 2013). In Nha Trang, Vietnam, the conversion of forests and farmland has compromised carbon storage and erosion control, negatively affecting crop yields and ecosystem resilience (Pham & Lin, 2023; Zambon *et al.*, 2018).

Agricultural systems are particularly vulnerable to sealing-related land conversion. High-quality agricultural soils, typically classified under USDA Classes 1 to 3, are frequently targeted for development due to their favorable topographic and logistic conditions (Andrade *et al.*, 2022; McGrane, 2016; Seifollahi-Aghmuni *et al.*, 2022). Soils with low compaction resistance are especially susceptible to sealing-induced degradation, including increased runoff, erosion, and nutrient losses (Clunes *et al.*, 2022). Disruptions to hydrological and nutrient cycles often extend beyond sealed areas, generating off-site impacts in surrounding agricultural lands (Chen *et al.*, 2013; Deasy *et al.*, 2009; Thomas *et al.*, 2016).

Despite the urgency, existing methodologies for assessing land degradation are not well-suited for predicting soil sealing vulnerability. Models like RUSLE focus on water erosion and omit urban planning variables such as zoning or infrastructure proximity (Gardi *et al.*, 2015). Land use change models provide valuable projections but operate at coarse spatial resolutions (~1 km), limiting their relevance for parcel-level planning in fragmented agricultural landscapes (Artmann, 2014; Terán-Gómez *et al.*, 2025). Similarly, the CORINE Land Cover-based model by Aksoy *et al.* (2017), with a minimum mapping unit of 25 hectares, cannot adequately represent areas like Valle del Cauca, where 43% of agricultural plots are smaller than 10 hectares (CVC & IGAC, 2023). These limitations obscure critical local drivers of soil sealing risk, including slope, soil type, and tenure status.

Conceptual frameworks linking ecosystem services with spatial drivers, such as those proposed by Assennato *et al.* (2022), offer valuable insights but often omit soil-specific attributes like compaction resistance or agrological classification. Moreover, they tend to be retrospective, focusing on the impacts of sealing rather than predictive vulnerability. For instance, Xiao *et al.* (2013) assessed landscape fragmentation in Hangzhou Bay post-sealing using spatial indices but offered little guidance for proactive zoning or soil conservation. Importantly, most existing models underperform in regulatory contexts where land-use decisions are governed by statutory planning instruments (e.g., municipal land-use plans) and environmental determinants that legally delimit developable land. Frameworks that omit these instruments often fail to anticipate where sealing pressure will be authorized in practice, even when biophysical suitability is high.

This regulatory gap is particularly acute in Colombia's Valle del Cauca, a region with high concentrations of fertile soils and growing urban pressures. Although it contains over 13% of Colombia's Class 1 and 2 agricultural soils, the department experienced a >30% increase in urbanized area from 2000 to 2020 (CVC & IGAC, 2023). Municipalities such as Palmira and Candelaria illustrate mounting tensions between conservation goals and development agendas, exacerbated by inconsistent enforcement and fragmented planning.

In Colombia, existing vulnerability assessments rarely combine agrological classification with legal land-use designations such as POTs, or operate at scales appropriate for municipal planning. While several studies stress the importance of integrating soil capability with regulatory instruments, implementations remain limited (Ajmone-Marsan *et al.*, 2016; Artmann, 2015; Croci *et al.*, 2021).

These methodological and policy gaps motivate an integrated framework that (i) produces fine-resolution spatial outputs, (ii) combines biophysical and regulatory parameters, and (iii) informs forward-looking planning. Therefore, a Soil Sealing Vulnerability Index (SSVI) was developed for the Guachal and Amaime

watersheds (Valle del Cauca, Colombia) that integrates seven parameters—slope, parcel size, distance to roads, proximity to water bodies, agrological class, urban growth (2000–2024), and municipal land-use designations—within a GIS-based multi-criteria analysis using AHP-elicited expert weights. It is hypothesized that a spatially explicit vulnerability index, coupling biophysical factors with institutional planning instruments, will more effectively identify zones under elevated sealing pressure in peri-urban agricultural landscapes. Specifically, the study assesses whether municipal land-use planning designations (POTs) exhibit stronger spatial concordance with mapped vulnerability than biophysical parameters alone, and whether the integrated framework aligns with observed land-use changes without claiming predictive inference.

MATERIAL AND METHODS

The proposed methodological framework integrates Multi-Criteria Analysis (MCA), the Analytic Hierarchy Process (AHP), and Geographic Information Systems (GIS) to enable the spatial assessment of both qualitative and quantitative vulnerability parameters—an approach previously applied in diverse environmental contexts (Echeverri-Sánchez *et al.*, 2020; Hu *et al.*, 2023; Piero *et al.*, 2017; Terán-Gómez *et al.*, 2025).

Study area

The study area comprises 126,734.87 hectares distributed between the GAWs, located in the southeastern portion of Valle del Cauca, Colombia. This territory is administratively divided between two municipalities: Palmira, covering 100,497.28 ha, and Candelaria, with 26,262.23 ha (Figure 1, left). The elevation ranges from approximately 950 to 3,200 meters above sea level, with 74.3% of the area located below 1,000 m (primarily alluvial plains), 18.5% between 1,000 and 2,000 m (piedmont and foothills), and the remaining 7.2% above 2,000 m (Andean montane zones) (Figure 1, right).

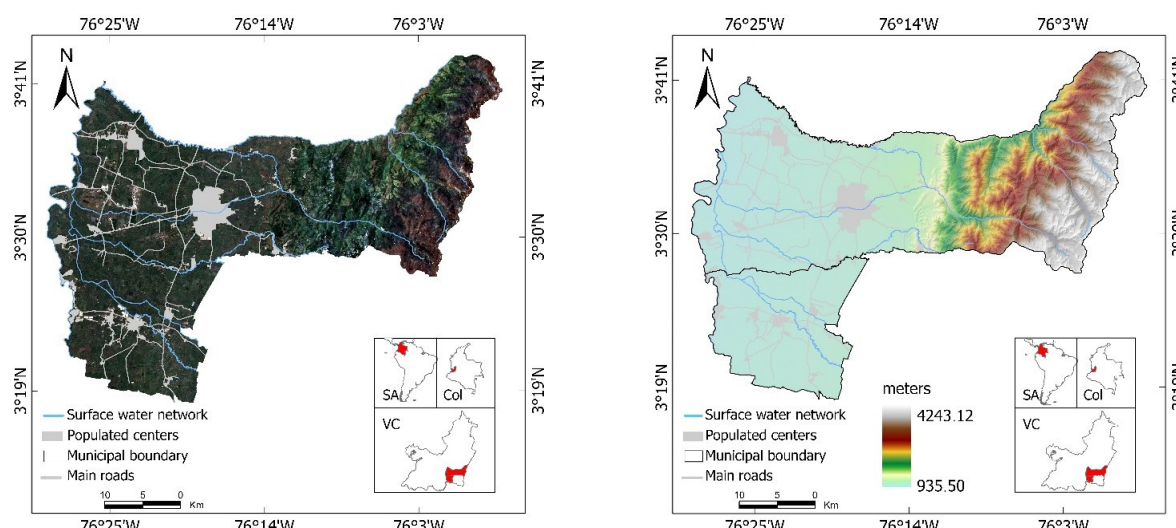


Figure 1: Study area. Left: true color composite; right: Digital elevation model; (SA: South America, Col: Colombia, VC: Valle del Cauca)

The region's climate ranges from tropical monsoon in the lowlands to humid subtropical in the uplands according to Köppen's climate classification, with annual rainfall between 950–1,700 mm and a bimodal distribution. Temperatures average 23–26°C in the valley and drop below 17°C in montane zones, shaping hydrology, soil formation, and agriculture (CVC & IGAC, 2023). Soils include Mollisols, Inceptisols, Vertisols, Andisols, Entisols, Alfisols, and Histosols. Mollisols, covering over 45% of agricultural land, dominate the valley due to high fertility. Inceptisols and Vertisols are found on slopes, whereas Andisols and Histosols are limited to volcanic uplands and poorly drained areas (CVC & IGAC, 2023), supporting both monocultures and diversified smallholder farming.

Land use in the study area is dominated by agriculture (62.4%), followed by secondary forests (15.3%), urban and peri-urban development (12.9%), and infrastructure or bare soil (9.4%) (DANE, 2023). Urban expansion is especially pronounced in Palmira and Candelaria, which together account for 10.9 trillion COP (~2.73 billion USD) in gross value added (2021). The department's total population reached 4,638,029 in 2023, and ongoing rural-to-urban migration is a key driver of spatial transformation. Projections suggest that, if current urbanization trends persist, sealed surfaces could increase by up to 35% by 2040 (DANE, 2023; own projection based on observed trends).

Economically, the area is a major agro-industrial and logistics hub. However, land price increases, infrastructure demand, and weak zoning enforcement heighten pressure on fertile soils. Environmental protections implemented by CVC include restrictions on converting Class 2, 3, and 8 soils, as well as buffer zones for rivers, páramos, and conservation areas (CVC, 2024).

Definition of vulnerability parameters

A systematic literature review identified biophysical and socioeconomic parameters commonly used in soil sealing vulnerability assessments (2008–2023), based on PRISMA guidelines and keyword searches in Scopus, Web of Science, and ScienceDirect. Selected studies applied spatially explicit methods and focused on peri-urban or agricultural contexts.

A panel of 18 experts—selected for their expertise in soil science, land use planning, territorial governance, and geospatial analysis within Valle del Cauca—participated in a three-round Delphi process (Mukherjee *et al.*, 2015). This process yielded a strong consensus (Kendall's $W = 0.82$, $p < 0.001$), ultimately retaining seven key parameters. These parameters were further validated through spatial comparison with observed sealing patterns from 2000 to 2024 and zoning data from municipal POTs. The final list, presented in Table 1, reflects both scientific precedent and empirical alignment with regional sealing dynamics, enhancing the robustness and replicability of the SSVI framework.

Table 1. Vulnerability parameters

Parameter	Summary
Distance to road network (DRN)	Proximity to roads increases sealing risk by attracting infrastructure and investment (Vieillard <i>et al.</i> , 2024).
Distance to surface water bodies (DSWB)	Areas near water bodies are more prone to land use change and sealing due to settlement and discharge needs (Pristeri <i>et al.</i> , 2020; Tóth <i>et al.</i> , 2022).
Terrain or topographic slope (TS)	Gentle slopes are favored for development due to lower construction costs, raising sealing vulnerability (Thomas <i>et al.</i> , 2016).
Urban growth trend (UGT)	Recent urban expansion patterns predict where future sealing pressures will concentrate (Beckers <i>et al.</i> , 2020; Karimi <i>et al.</i> , 2018; Stevenson <i>et al.</i> , 2025).
Soil agrological classes (SAC)	Soils not environmentally restricted are more exposed to development, varying by municipality and guided by Res. 0459 of 2024 (CVC).
Land parcel size (LPS)	Larger parcels, often held by wealthy owners, are more likely to transform (Peroni <i>et al.</i> , 2020).
Land use designations in municipal land-use plans (LU-POTs)	Municipal zoning plans directly indicate areas intended for future development and sealing (Artmann, 2015; Hurni <i>et al.</i> , 2015; Vieillard <i>et al.</i> , 2024).

Parameter categorization

After selecting the seven vulnerability parameters, each was classified into high, moderate, or low vulnerability using thresholds informed by expert judgment, institutional criteria, and regional planning norms. This process involved collaboration with technical staff from Corporación Autónoma del Valle del Cauca-CVC, researchers from Universidad del Valle, and references on land-use and soil conservation.

For example, the DRN threshold of 560 meters corresponds to the average parcel length reported by IGAC. TS categories (<7%, 7–25%, >25%) follow CVC's classification for construction feasibility. UGT thresholds reflect proximity to urban expansion fronts documented between 2000 and 2024, assigning higher vulnerability to areas closest to recent growth. These classifications reflect local planning realities and legal instruments such as Res. 0459 (CVC, 2024), ensuring practical application (Tables 2 and 3).

Table 2. Vulnerability categories per parameter

Parameter	Categories	Vulnerability
DRN	Less than 560 m	High
	Between 560 m and 1,120 m	Moderate
	Greater than 1,120 m	Low
DSWB	Less than 600 m	High
	Between 600 m and 1,200 m	Moderate
	Greater than 1,200 m	Low

Parameter	Categories	Vulnerability
TS	Less than 7%	High
	Between 7% and 25%	Moderate
	Greater than 25%	Low
UGT	Areas within the same distance as urban expansion observed in the past 24 years.	High
	Areas at twice the distance from expansion zones of the last 24 years.	Moderate
	Areas located at more than twice the distance from past expansion zones.	Low
SAC	Classes 6 and 7	High
	Classes 4 and 5	Moderate
	Classes 1, 2, 3, and 8	Low
LPS	Greater than 50 ha	High
	Between 10 and 50 ha	Moderate
	Less than 10 ha	Low
LU-POTs	Urban expansion zones	High
	Other designated uses	Low

Table 3. Criteria for categorizing vulnerability parameters

Parameter	Criteria	Categories
DRN	Based on the average land length established by IGAC around road infrastructure.	High: < 560 m Moderate: 560–1,120 m Low: > 1,120 m
DSWB	Based on the average land length established by IGAC around surface water sources.	High: < 600 m Moderate: 600–1,200 m Low: > 1,200 m
TS	Classification proposed by CVC, considering construction feasibility.	High: < 7% Moderate: 7–25% Low: > 25%
UGT	Derived from multi-temporal analysis of urban expansion.	High: Areas within the same distance as expansion observed over the past 24 years. Moderate: Areas at twice the distance from past expansion zones. Low: Areas beyond twice the distance from past expansion zones.
SAC	Based on the ED established in CVC Res. 0459. Vulnerability categories are assigned per municipality.	Categories defined per municipality according to Colombian law
LPS	Low vulnerability corresponds to small rural properties (<10 ha). A fixed threshold of 50 ha is proposed between Moderate and high vulnerability, based on the absence of specific area definitions in POTs.	High: > 50 ha Moderate: 10–50 ha Low: < 10 ha
LU-POTs	Municipal POTs define future land-use designations.	High: Areas designated for urban expansion and associated uses Low: Areas not designated for expansion-related uses

Although thresholds were not derived from empirical comparisons (e.g., sealed vs. unsealed zones), they reflect context-appropriate criteria rooted in institutional planning. No Receiver Operating Characteristic, Jenks natural breaks, or Area Under the Curve validation was performed. Despite this, the framework remains operationally valid for policy use in Valle del Cauca.

Weight definition

The AHP method (Saaty, 2013) was used to assign weights to the seven vulnerability parameters through pairwise comparisons by experts using Saaty's 1–9 scale. Aggregated judgments formed a group decision matrix, with internal consistency confirmed (CR = 2.51%; CI = 3.3%), well below the 10% threshold. Among evaluators, LU-POTs ranked in the top two for 66.7%, followed by UGT (44.4%), SAC (33.3%), and LPS (27.7%). Conversely, DSWB received the lowest score from 77.7% of experts, and TS ranked among the two lowest for 61.1%. Full results are summarized in Table 4.

Table 4. Weights assigned to vulnerability parameters

Parameter	Weight (%)	Rank
LU- POTs	32.30%	1
UGT	23.80%	2
LPS	12.10%	3
SAC	9.70%	4
DRN	8.80%	5
TS	7.00%	6
DSWB	6.30%	7
Total	100.00%	

Parameter normalization

To enable multi-criteria integration, all parameter categories were normalized to a 0–1 scale, allowing heterogeneous variables to be combined in a weighted overlay. Each parameter was classified into three ordinal vulnerability categories—High, Moderate, and Low—assigned normalized values of 1.0, 0.66, and 0.33, respectively, reflecting expert consensus and standard GIS-MCDA practice. This approach ensures maximum vulnerability is represented by 1.0, while the lowest is set at 0.33 to avoid zero-weighting and maintain proportionality.

Category assignments for each parameter were based on legal, institutional, or empirical thresholds, with a summary of all parameter weights, categories, and normalized values provided in Table 5.

Table 5. Normalized values of categories by vulnerability parameter

Parameter	Weight (%)	Vulnerability Category	Normalized Value
LU-POTs	32.30%	High	1
		Low	0.33
UGT	23.80%	High	1
		Moderate	0.66
LPS	12.10%	Low	0.33
		High	1
		Moderate	0.66
		Low	0.33

Parameter	Weight (%)	Vulnerability Category	Normalized Value
SAC	9.20%	High	1
		Moderate	0.66
		Low	0.33
DRN	8.80%	High	1
		Moderate	0.66
		Low	0.33
TS	7.00%	High	1
		Moderate	0.66
		Low	0.33
DSWB	6.30%	High	1
		Moderate	0.66
		Low	0.33

Finally, the official information sources are presented in Table 6.

Table 6. *Information sources*

Parameter	Official source	Format	Description
DRN	INVIAS	Vector	Line layer representing road types
DSWB	GEOCVC	Vector	Line layer showing hydrographic network (rivers, streams, and drainage channels)
TS	CVC	Vector	Digital elevation model (2.5 × 2.5 m spatial resolution)
UGT	Contract 0792 of 2024	Raster	Layers of sealed areas in the study zone from 2000 to 2024
SAC	CVC and IGAC (2023). Semi-detailed soil survey of Valle del Cauca	Vector	Polygon layer representing soil capability classes (agrological classification)
LPS	IGAC Cartography	Vector	Polygon layer of land parcels within the study area
LU-POTs	Municipality of Palmira, Municipality of Candelaria	Vector	Polygon layers of land use as defined in municipal POTs

INVIAS: National Roads Institute (Colombia); GEOCVC: Public geographic information systems portal of the CVC; CVC: Corporación Autónoma Regional del Valle del Cauca; IGAC: Agustín Codazzi Geographic Institute (Colombia). Regulatory layers include municipal POTs and the departmental environmental determinants issued by CVC (Res. 0459/2024), used as data inputs. All layers integrated at 2.5 × 2.5 m; vectors rasterized; UGT (Contract 0792/2024) compiled from multi-sensor imagery and integrated at 2.5 m; native map scales vary and are not uniformly reported.

SSVI mapping

The Simple Additive Weighting method (Kaliszewski & Podkopaev, 2016; Taherdoost, 2023) was adapted for the spatial distribution of results, and then it was applied to map the SSVI. The general expression applied is presented in Equation 1.

$$SSVI = \sum_{i=1}^n (w_i VN_i) \quad (\text{Equation 1})$$

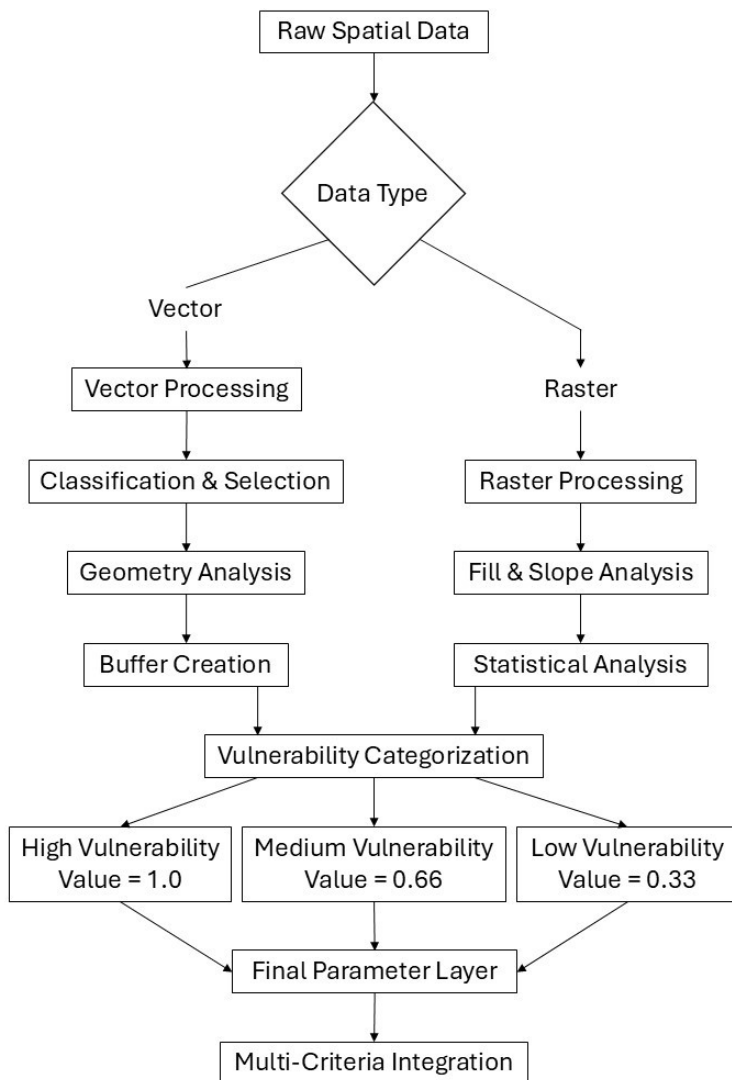
Where W : Weight of vulnerability parameter I and VN : Normalized value of vulnerability parameter i.

This approach generated an SSVI value for each pixel within the study area, enabling identification of homogeneous zones using index value ranges.

GIS processing

For each parameter, geospatial tools in ArcGIS Pro 3.5 (ESRI, USA) were used to clip, classify, project, and create buffer zones, targeting areas of highest vulnerability based on site-specific conditions. All data were processed in the MAGNA Colombia West coordinate system, with vector and raster layers standardized to the study area using the Clip and Extract by Mask tools. The overall workflow is summarized in Figure 2. All inputs were harmonized to a 2.5×2.5 m raster grid, anchored to the official DEM at the same resolution. Vector sources (roads, drainage, planning/zoning) were rasterized onto this grid to minimize sub-cell aliasing and to preserve narrow linear features during weighted overlay. This cell size balances feature fidelity and computational tractability for the study extent.

Figure 2: GIS workflow followed to estimate the SSVI at the GAWs



RESULTS

Vulnerability parameter maps and integrated vulnerability assessment

The vulnerability maps for each parameter are presented, followed by exclusion zone maps that define areas where vulnerability analysis is not applicable due to constraints such as existing urban footprints, protected natural areas, and regulatory water buffers. Finally, the SSVI map and homogeneous vulnerability zones are presented, estimated using the previously defined SSVI ranges.

Individual parameter vulnerability maps

Land use planning parameter. The vulnerability map based on the LU-POTs parameter for the municipalities of Palmira and Candelaria is presented in Figure 3a. This analysis utilized the most current available POTs. Areas designated for future expansion projects are highlighted in red, representing High Vulnerability zones. These zones are predominantly located in the flat terrain of both municipalities, near existing urban areas. Recreational real estate zones constitute an intermediate category, classified as Moderate Vulnerability. All remaining areas are classified as Low Vulnerability.

Urban growth trend parameter. The vulnerability map for the UGT parameter, based on multitemporal analysis conducted within the framework of this study, is presented in Figure 3b. Red zones identify areas in the closest proximity to regions urbanized during the past 24 years, categorized as High Vulnerability. These high-vulnerability zones are spatially associated with current urban centers (both primary and secondary). Yellow zones represent areas adjacent to high-vulnerability zones, classified as Moderate Vulnerability, while the remainder of the study area is classified as Low Vulnerability.

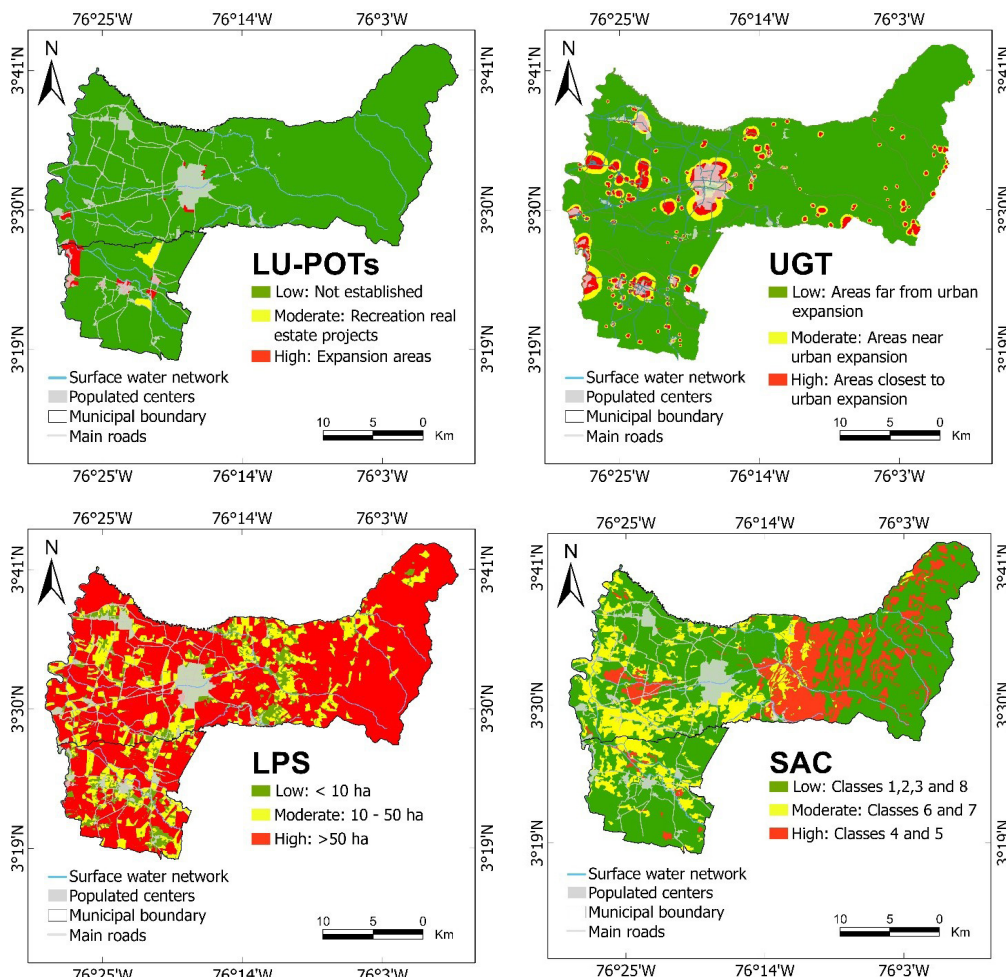
Land parcel size parameter. The vulnerability map for the LPS parameter is illustrated in Figure 3c. Red zones (High Vulnerability) clearly correspond to properties exceeding 50 hectares, distributed throughout the study area (both flat and sloped terrain). Yellow zones (Moderate Vulnerability) represent properties ranging from 10 to 50 hectares, similarly distributed across the study area. Green zones (Low Vulnerability) correspond to properties ≤ 10 hectares, primarily situated in flat terrain and on the western slope of the Central range Central Cordillera.

Soil agrological classes parameter. The vulnerability map for SAC is presented in Figure 3d. Green zones represent agrological classes 2, 3, and 8, classified as Low Vulnerability. For these municipalities, these agrological classes are considered in CVC's ED (Res. 0459). These areas are primarily located in flat terrain (Classes 2 and 3) and high-elevation zones (Class 8). Yellow zones (Moderate Vulnerability) correspond to agrological classes 6 and 7, located in flat terrain and piedmont areas. Red zones (High Vulnerability) represent agrological classes 4 and 5, primarily located in flat terrain with minimal presence in piedmont areas.

Distance to road network parameter. The vulnerability map for the DRN parameter is displayed in Figure 3e. Red and yellow zones (High and Moderate Vulnerability, respectively) are in flat terrain areas with primary and secondary roads susceptible to urban sprawl or industrial development.

Terrain slope parameter. The vulnerability map for the TS parameter is presented in Figure 3f. Green zones (Low Vulnerability) represent areas with slopes >25%, located on the Eastern Cordillera. Yellow zones (Moderate Vulnerability) represent areas with slopes between 7-25%, located in piedmont areas and some high-elevation zones of the Eastern Cordillera. Red zones represent the flattest areas (slopes <7%), indicating high vulnerability to urban expansion and infrastructure development processes. These areas are in the geographical valley of the Cauca River (eastern margin).

Distance to surface water sources parameter. The vulnerability map for the DSWS parameter is presented in Figure 3g. This map displays two buffer zones around rivers, streams, and drainage channels in the study area. The vulnerability category distribution is determined by the spatial distribution of the considered hydrographic network.



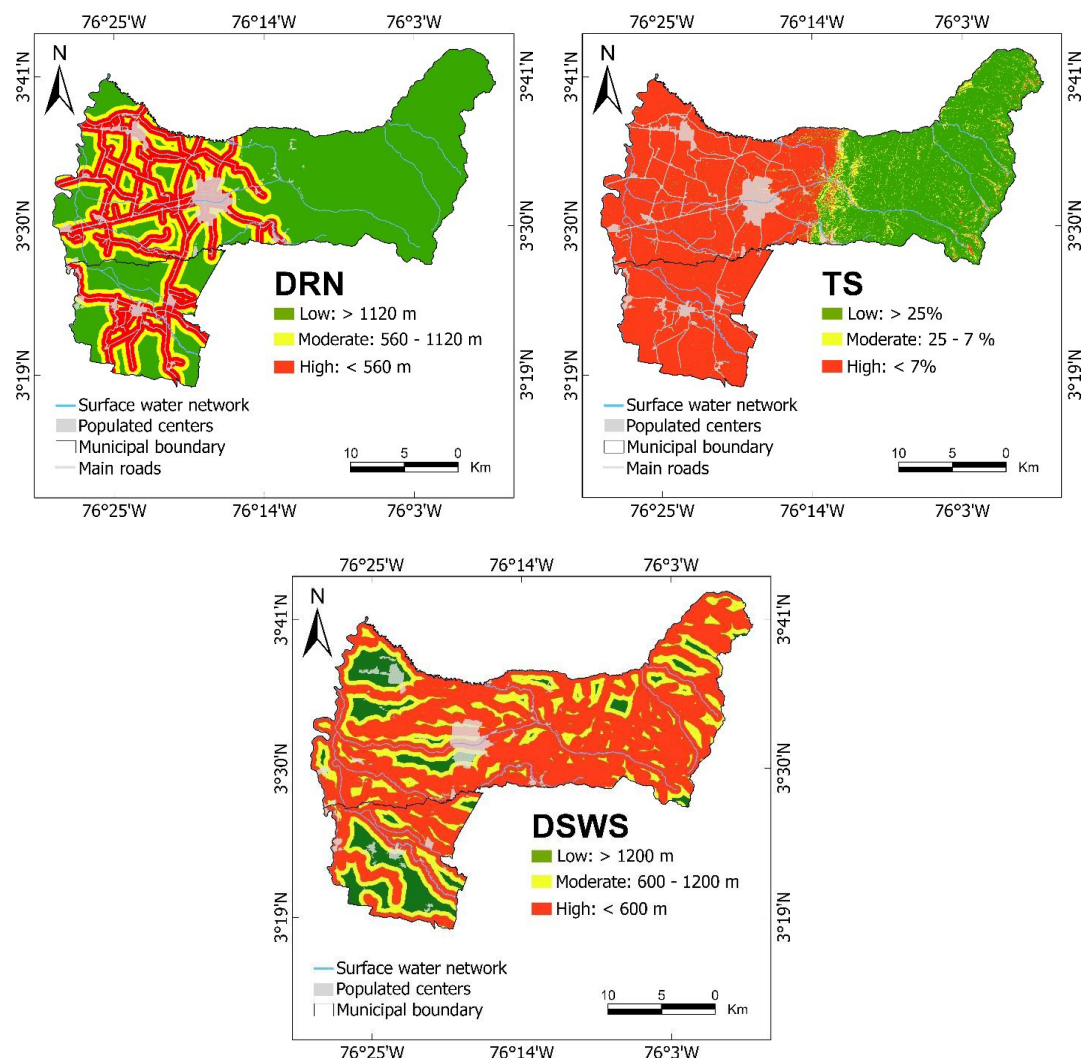


Figure 3: Vulnerability parameter maps and integrated vulnerability assessment: a) Land use planning; b) Urban growth trend; c) Land parcel size; d) Soil agrological classes; e) Distance to road network; f) Terrain slope; g) Distance to surface water sources.

Exclusion zones. As part of this analysis, the need to define exclusion zones was identified, understood as areas where vulnerability analysis is not applicable due to existing urban settlements, protected environmental areas, and mandatory hydrological buffer zones. Specifically, these exclusion zones included: current urban centers, water source protection zones, and protected areas (Figures 4a, 4b, and 4c). The protected areas considered were: National Natural Parks, National Forest Reserves, and Natural Resource Reserves. Pixels belonging to exclusion zones were assigned a value of 1; thus, when multiplying these raster layers by parameter layers and their weights, values in pixels not belonging to exclusion zones remain unaltered.

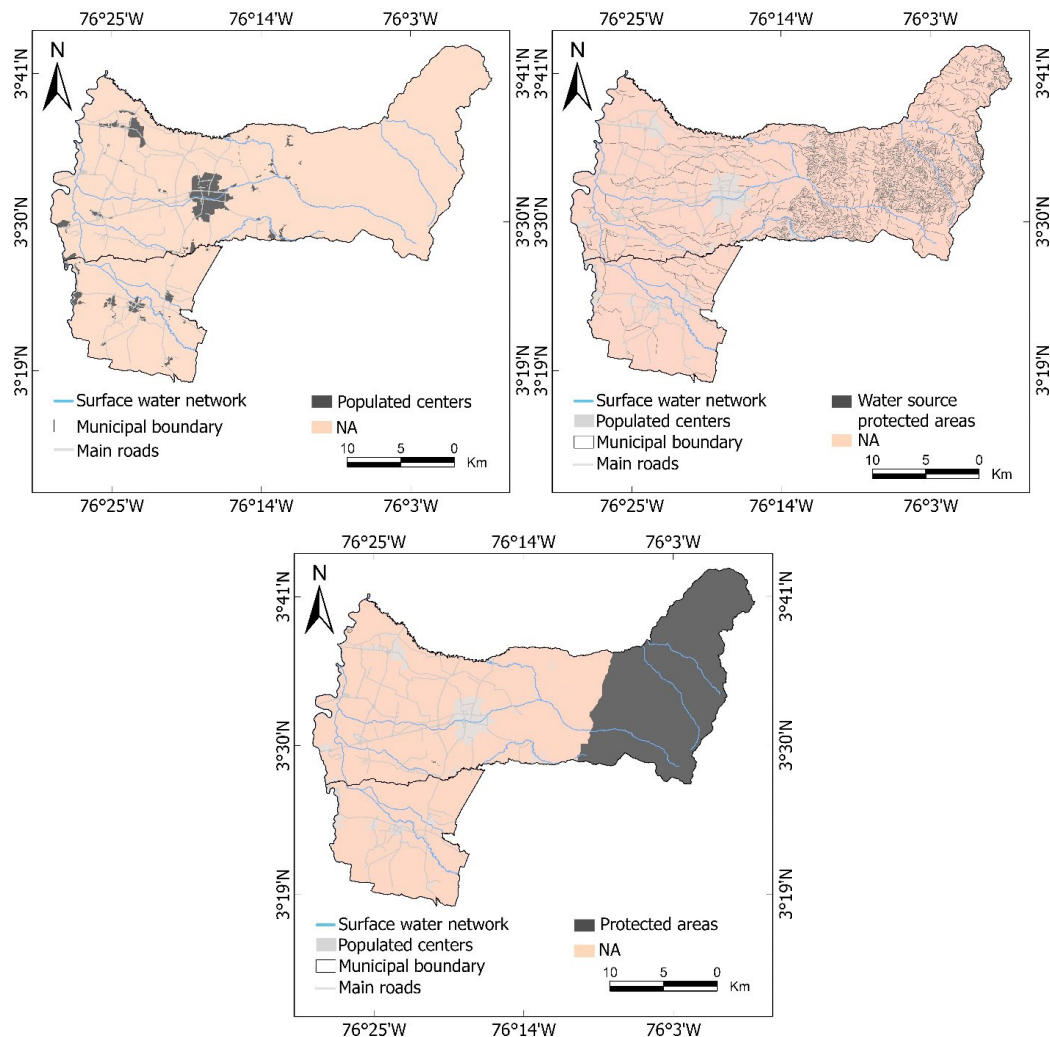


Figure 4: Exclusion zones: a) Exclusion zones due to current urban centers; b) Exclusion zones due to water source protected areas (river's buffer distance: 30 m); c) Exclusion zones due to protected areas (for instance, Páramos).

SSVI Integration. The SSVI was calculated as a weighted sum of normalized parameters, integrated with an exclusion mask to remove protected or non-developable areas. The correct formulation of the index is shown in Equation 2:

$$\begin{aligned}
 SSVI = & [(0.323 \times LU_{POTS}) + (0.238 \times UGT) + (0.121 \times LPS) + (0.097 \times SAC) \\
 & + (0.088 \times DRN) + (0.070 \times TS) + (0.063 \times DSWB)] \times Mask
 \end{aligned} \quad (\text{Equation 2})$$

Where Mask is a binary layer (1 = analysis zone; 0 = exclusion zone), and each component corresponds to a normalized parameter raster. The highest SSVI values are concentrated in the flatlands of the Cauca River Valley, primarily associated with existing urban areas (Figures 5a, 5b, 5c, and 5d).

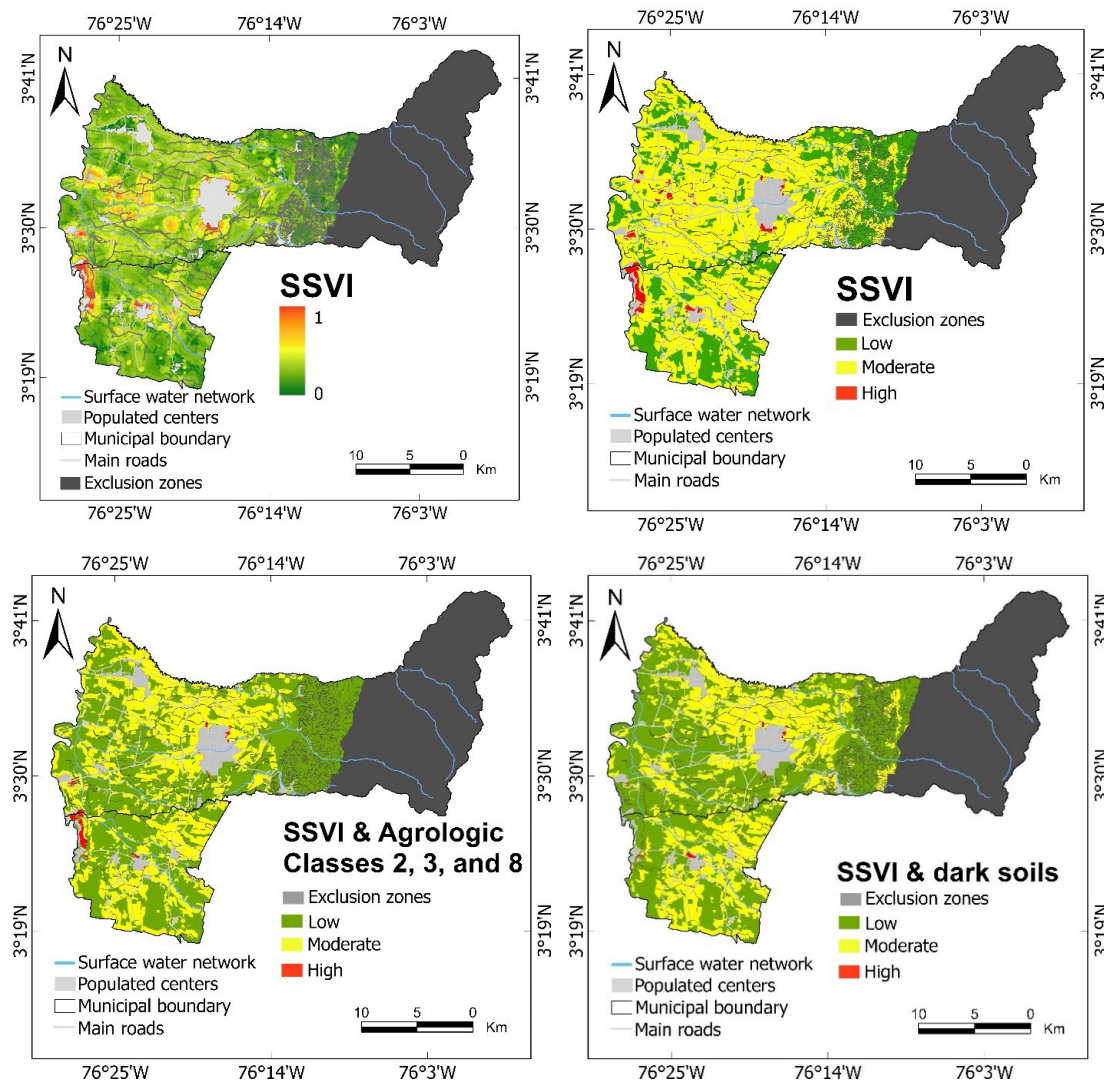


Figure 5: SSVI integration: a) Soil Vulnerability Index to Surface Sealing; b) Homogeneous zones of soil vulnerability to surface sealing; c) Homogeneous zones of SSVI vs Agrologic Classes 2, 3, and 8; d) Homogeneous zones of SSVI.

In addition, Table 7 presents the total area corresponding to each vulnerability category across the study area. The high vulnerability zones clearly align with areas designated for urban expansion in the municipal POTs. These zones are typically located on gentle slopes, in proximity to primary roads, on Moderate to large parcels, and within agrological classes 4 or 5.

Table 7. Normalized values of categories by vulnerability parameter

Category	Area (ha)	% of Total Area
Exclusion zones	47,334.80	37.44%
Low	24,027.80	19.01%
Moderate	53,780.40	42.54%
High	1,270.10	1.00%
Total	126,413.10	100.00%

To evaluate the relative vulnerability of different soil agrological classes to surface sealing, a spatial intersection analysis between the SSVI map and the agrological classification layer was conducted. Table 8 presents the total area occupied by each agrological class within the three vulnerability categories—Low, Moderate, and High. However, raw area values alone are insufficient to assess relative risk across soil types. Therefore, the percentage distribution of vulnerability levels within each soil class to facilitate comparative analysis was computed.

Table 8. Area (ha) by agrological class and vulnerability category (excluding water bodies and artificial areas)

Category	Class 2	Class 3	Class 4	Class 6	Class 7	Class 8
Exclusion zones	25.2	1,423.20	1,155.20	5,971.50	4,876.20	27,035.80
Low	497.3	13,942.20	2,883.90	1,194.50	1,656.00	2,022.30
Moderate	607.9	30,298.70	15,052.40	4,353.50	2,150.60	20.5
High	543.7	388.2	62	93.4	8.3	6.8
Total	1,674.10	46,052.20	19,153.50	11,613.00	8,691.10	29,085.40

For Class 2 soils, which are among the most fertile and environmentally protected according to CVC's Res. 0459, 32.5% are classified as High vulnerability, 36.3% as Moderate, and 29.7% as Low. Similarly, Class 3 soils show 0.8% in High, 65.8% in Moderate, and 30.3% in Low vulnerability. For Class 8 soils, typically found on steep slopes and also protected, 0.02% fall under High vulnerability, while 0.07% fall under Moderate vulnerability. Although the high vulnerability percentages in Class 3 and 8 soils are numerically low, the total exposed area remains ecologically significant due to their extent and protection status.

To describe over- or under-representation of the “High” category by soil class, a High-Designation Enrichment (HDE) was computed as the percentage of each soil class mapped as High divided by the overall percentage of High in the study area (1.00%). For Class 2 soils, 543.7 ha of 1,674.1 ha are mapped as High (32.5%), yielding HDE = 32.5, i.e., a 32.5-fold enrichment of area labeled High relative to the study-wide baseline. For Class 3, 388.2 ha of 46,052.2 ha are High (0.84%), giving HDE = 0.84, indicating slight under-representation. These enrichment values are area-based descriptors of how the “High” designation concentrates within soil classes; they do not imply intrinsic, per-parcel risk or causality.

Additionally, an intersection between the homogeneous vulnerability zones map and the dark fertile soil taxonomic orders (Mollisols, Andisols, and Histosols) resulted in the data presented in Figure 5d and Table 9.

Table 9. Area (ha) by soil taxonomic order and vulnerability category.

Taxonomic order	Exclusion Zones	Low	Moderate	High	Exposed area (ha)*	Total area (ha)
Alfisol	109.8	45.3	1,298.10	45.5	1,388.9	1,498.7
Andisol	20,817.3	23.6	168	0	191.6	21,008.9
Entisol	1,126.3	157.8	128.7	0.2	286.7	1,413.0
Histosol	2,425.1	0	0	0	0	2,425.1
Inceptisol	4,042.6	4,146.5	5,674.7	385.2	10,206.4	14,249.0
Mollisol	11,556.8	15,268.3	30,560.0	228.8	46,057.1	57,613.9
Vertisol	409.0	2,554.5	14,654.2	427.7	17,636.4	18,045.4
Total	40,486.9	22,196.0	52,483.7	1,087.4	75,767.1	116,254.0

*Exposed area = Low + Moderate + High (excludes Exclusion Zones).

Uncertainty and Consistency Assessment. The SSVI exhibited strong internal consistency (group CR = 2.51%, <10% threshold). For an ex post, non-independent concordance verification, areas classified as High in 2018 (threshold ≥ 0.75) were intersected with an institutional compilation of sealing outcomes for 2018–2023 (Contract 0792 of 2024). An 85.2% spatial overlap was observed. Because the 2018 ‘urban growth’ parameter and the 2018–2023 sealing layers share institutional provenance, this overlap reflects program-internal consistency rather than predictive validation. All parameters were processed on a 2.5×2.5 m grid to align with the official DEM and retain narrow linear features when rasterizing vector inputs; remaining uncertainties arise from input resolution, expert-judgment variability, and edge effects near exclusion zones. A formal error-propagation analysis (e.g., Monte Carlo) was not performed and remains future work.

DISCUSSION

The spatial distribution of soil sealing vulnerability in the GAWs highlights the interplay between biophysical conditions, territorial governance, and development pressures. Most of the study area falls under Moderate and Low vulnerability, indicating general resistance to sealing, whereas only 1.00% is classified as highly vulnerable. Although this proportion is small, it includes land of exceptional agronomic and ecological value—specifically, 938.7 hectares of environmentally restricted soils (agrological classes 2, 3, and 8) and 228.8 hectares of fertile Mollisols.

High-vulnerability zones are strategically located, concentrated in flat terrain near existing population centers and major infrastructure. This pattern aligns with observations from Mediterranean contexts (Zambon *et al.*, 2018), where similarly defined zones are also found near urban and infrastructural nodes. The dominant influence of planning-related parameters—POTs and urban growth trends together accounting for 56.1% of the index—explains the spatial concentration of high

vulnerability in areas where planned expansion overlaps with optimal development conditions, such as flat topography, large parcels, and road proximity. This convergence suggests that planning instruments in Valle del Cauca may be steering urban expansion into areas that are both accessible and agriculturally valuable.

Independent validation is not yet possible due to the absence of sealing datasets external to the inputs used here. Of the estimated 2,340 ha sealed between 2000 and 2024, 68% of intersected cells were classified as High or Moderate at the time of mapping; the remaining 32% occurred in cells classified as Low or in Exclusion Zones outside the modeled decision space. Therefore, this *ex post* overlap indicates program-internal concordance, not an independent predictive validation. For context, the study area comprises 37.44% Exclusion Zones, 19.01% Low, 42.54% Moderate, and 1.00% High, which constrains the maximum possible intersection with High/Moderate classes. The Simple Additive Weighting (SAW) formulation imposes linearity and additivity, potentially under-representing non-linear or multiplicative interactions; future work could explore fuzzy logic or machine-learning frameworks to better capture such dynamics (Hastings *et al.*, 2020; Forkuor *et al.*, 2017).

Other limitations relate to spatial and temporal inconsistencies. The 2.5×2.5 -meter resolution may obscure finer-grained variability in soil properties or parcel-level planning decisions, and temporal mismatches between parameter layers—such as urban growth data (2000–2024), soil surveys (2023), and POTs (2019–2022)—may introduce systematic uncertainty, potentially altering vulnerability profiles by an estimated 15–20% over time. Moreover, the exclusion of 37.44% of the territory due to urban, protected, or other land uses limits the model's applicability in fully comprehensive planning contexts and may omit critical interface zones where urban-agricultural conflict is most acute.

Bias in expert input is also a concern, as all panel members were based in Colombian institutions, potentially reducing model transferability to other regions. While the resulting CR of 2.51% supports internal coherence in expert judgment, underlying uncertainties in parameter values or categorization thresholds remain. These cumulative uncertainties underscore the need for a more robust uncertainty propagation framework, such as Monte Carlo simulation, to assess the range of plausible model outcomes.

Despite these limitations, the SSVI offers an actionable, scientifically grounded tool for guiding land use policy. Its ability to translate complex, multidimensional data into spatially explicit decision-support layers can enhance zoning transparency and enforceability, as supported by GIS-based policy strategies. Periodic updating of the SSVI in response to urban growth, regulatory changes, and land cover trends can further refine its policy relevance. Replication in other regions with similar socio-environmental pressures—such as the Bogotá highlands or the Coffee belt—is feasible due to the model's flexible structure.

The identification of high-vulnerability zones within agriculturally strategic soils constitutes a call to action for policymakers and planners. Institutionalizing tools like the SSVI into municipal and regional planning workflows offers a pragmatic pathway toward aligning development trajectories with long-term sustainability objectives. Future research should prioritize dynamic modeling frameworks, governance responsiveness analysis, and economic impact assessments to support integrated land management under intensifying urbanization pressures.

CONCLUSIONS

The SSVI demonstrates that combining multi-criteria GIS analysis with expert-informed weighting enables fine-scale identification of sealing vulnerability in agricultural frontiers. With strong internal consistency (CR = 2.51%) and strong internal coherence (CR = 2.51%), an ex post concordance verification suggested high overlap with subsequently sealed areas within the same institutional compilation, but this does not constitute independent validation.

Municipal planning instruments, particularly land use designations in POTs, were the strongest predictors of vulnerability (32.3% of total index weight), surpassing biophysical factors like slope or water proximity. This highlights the critical role of zoning enforcement, regulatory coherence, and institutional capacity in soil conservation efforts—policy domains that require urgent strengthening.

Despite environmental restrictions such as municipal conservation zoning and protected soil designations, 938.7 ha of protected soils and 228.8 ha of fertile Mollisols fall within high-vulnerability zones. These findings point to enforcement gaps and the limitations of static legal designations. In order to close the implementation gap, the adoption of flexible policy tools such as conservation easements, payment for ecosystem services, and regulatory offsets should be explored.

The model's success depends on access to high-resolution spatial layers and localized expert input. Broader implementation will require formal integration into land-use instruments (e.g., revised POTs) and regular updates as urban growth and land use evolve. The flexible structure of the SSVI supports replication in other high-pressure agricultural zones, providing a scalable platform for sustainable territorial governance.

ACKNOWLEDGMENTS

The authors wish to express their sincere gratitude to the Corporación Autónoma Regional del Valle del Cauca (CVC) and the Universidad del Valle for their institutional support. This research was funded through Inter-Administrative Contract No. 0792 of 2024 (Project Code 42061F), established between CVC and the Universidad del Valle.

CONFLICT OF INTEREST

The authors declare that there is no conflict of interest.

REFERENCES

Ajmone-Marsan, F.; Certini, G.; Scalenghe, R. (2016). Describing urban soils through a faceted system ensures more informed decision-making. *Land Use Policy*. 51: 109–119. <https://doi.org/10.1016/j.landusepol.2015.10.025>

Andrade, J. F.; Cassman, K. G.; Rattalino Edreira, J. I.; Agus, F.; Bala, A.; Deng, N.; Grassini, P. (2022). Impact of urbanization trends on production of key staple crops. *Ambio*. 51: 1158–1167. <https://doi.org/10.1007/s13280-021-01674-z>

Aksoy, E.; Gregor, M.; Schröder, C.; Löhnertz, M.; Louwagie, G. (2017). Assessing and analysing the impact of land take pressures on arable land. *Solid Earth*. 8(3): 683–695. <https://doi.org/10.5194/se-8-683-2017>

Artemann, M. (2014). Assessment of soil sealing management responses, strategies, and targets toward ecologically sustainable Urban land use management. *Ambio*. 43(4): 530–541. <https://doi.org/10.1007/s13280-014-0511-1>

Artemann, M. (2015). Managing urban soil sealing in Munich and Leipzig (Germany)-From a wicked problem to clumsy solutions. *Land Use Policy*. 46: 21–37. <https://doi.org/10.1016/j.landusepol.2015.02.004>

Assennato, F.; Smiraglia, D.; Cavalli, A.; Congedo, L.; Giuliani, C.; Riiatto, N.; Strollo, A.; Munafò, M. (2022). The Impact of urbanization on land: A biophysical-based assessment of ecosystem services loss supported by remote sensed indicators. *Land*. 11(2). <https://doi.org/10.3390/land11020236>

Assouline, S.; Mualem, Y. (2002). Infiltration during soil sealing: The effect of areal heterogeneity of soil hydraulic properties. *Water Resources Research*. 38(12): 22-1-22-29. <https://doi.org/10.1029/2001WR001168>

Beckers, V.; Poelmans, L.; Van Rompaey, A.; Dendoncker, N. (2020). The impact of urbanization on agricultural dynamics: A case study in Belgium. *Journal of Land Use Science*. 15(5): 626–643. <https://doi.org/10.1080/1747423X.2020.1769211>

Chen, L.; Sela, S.; Svoray, T.; Assouline, S. (2013). The role of soil-surface sealing, microtopography, and vegetation patches in rainfall-runoff processes in semiarid areas. *Water Resources Research*. 49(9): 5585–5599. <https://doi.org/10.1002/wrcr.20360>

Clunes, J.; Valle, S.; Dörner, J.; Martínez, O.; Pinochet, D.; Zúñiga, F.; Blum, W. E. H. (2022). Soil fragility: A concept to ensure a sustainable use of soils. *Ecological Indicators*. 139. <https://doi.org/10.1016/j.ecolind.2022.108969>

Croci, E.; Lucchitta, B.; Penati, T. (2021). Valuing ecosystem services at the urban level: A critical review. *Sustainability*. 13(3): 1129. <https://doi.org/10.3390/su13031129>

CVC; IGAC. (2023). Levantamiento Semidetallado de Suelos del Departamento del Valle del Cauca Escala 1:25.000. <https://ecopedia.cvc.gov.co/suelo/caracteristicas-del-suelo/levantamiento-semidetallado-de-suelos-del-departamento-del-valle>

CVC. (2024). Resolución 0100 No. 0600-0459 de 2024. <https://www.cvc.gov.co/sites/default/files/2025-01/Resoluci%C3%B3n%200100%20No.%200600-0459%20de%202024%20Se%20expide%20determinantes%20ambientales%20a%20escala%20departamental%2odel%20medio%20transformado.pdf>

Dadi, W.; Mulegeta, M.; Simie, N. (2022). Urbanization and its effects on income diversification of farming households in Adama district, Ethiopia. *Cogent Economics and Finance*. 10(1). <https://doi.org/10.1080/23322039.2022.2149447>

Deasy, C.; Brazier, R. E.; Heathwaite, A. L.; Hodgkinson, R. (2009). Pathways of runoff and sediment transfer in small agricultural catchments. *Hydrological Processes*. 23(9): 1349–1358. <https://doi.org/10.1002/hyp.7257>

DANE. (2023). Información sobre el Departamento del Valle del Cauca. <https://www.dane.gov.co/files/investigaciones/planes-departamentos-ciudades/pres-ValleDelCauca-18Jul2023.pdf>

Echeverri-Sánchez, A. F.; Urrutia-Cobo, N.; Barona-Ramírez, S. M. (2020). Vulnerabilidad de fuentes hídricas superficiales de la cuenca del río cerrito a la contaminación difusa agrícola. *Revista de Investigación Agraria y Ambiental*. 11(2): 117–130. <https://doi.org/10.22490/21456453.3136>

Forkuor, G.; Hounkpatin, O. K. L.; Welp, G.; Thiel, M. (2017). High resolution mapping of soil properties using Remote Sensing variables in south-western Burkina Faso: A comparison of machine learning and multiple linear regression models. *PLOS ONE*. 12(1): 1–21. <https://doi.org/10.1371/journal.pone.0170478>

Gardi, C.; Panagos, P.; Van Liedekerke, M.; Bosco, C.; De Brogniez, D. (2015). Land take and food

security: assessment of land take on the agricultural production in Europe. *Journal of Environmental Planning and Management*. 58(5): 898–912. <https://doi.org/10.1080/09640568.2014.899490>

Garschagen, M.; Romero-Lankao, P. (2015). Exploring the relationships between urbanization trends and climate change vulnerability. *Climatic Change*. 133(1): 37–52. <https://doi.org/10.1007/s10584-013-0812-6>

Hastings, F.; Fuentes, I.; Perez-Bidegain, M.; Navas, R.; Gorgolione, A. (2020). Land-Cover Mapping of Agricultural Areas Using Machine Learning in Google Earth Engine. *Lecture Notes in Computer Science*. 12252: 721–736. https://doi.org/10.1007/978-3-030-58811-3_52

Hu, W.; Cichota, R.; Beare, M.; Müller, K.; Drewry, J.; Eger, A. (2023). Soil structural vulnerability: Critical review and conceptual development. *Geoderma*. 430. <https://doi.org/10.1016/j.geoderma.2023.116346>

Hurni, H.; Giger, M.; Liniger, H.; Mekdaschi Studer, R.; Messerli, P.; Portner, B.; Schwilch, G.; Wolfgramm, B.; Breu, T. (2015). Soils, agriculture and food security: The interplay between ecosystem functioning and human well-being. *Current Opinion in Environmental Sustainability*. 15: 25–34. <https://doi.org/10.1016/j.cosust.2015.07.009>

Kaliszewski, I.; Podkopaev, D. (2016). Simple additive weighting—A metamodel for multiple criteria decision analysis methods. *Expert Systems with Applications*. 54: 155–161. <https://doi.org/10.1016/j.eswa.2016.01.042>

Karimi, M.; Nazari, R.; Dutova, D.; Khanbilvardi, R.; Ghandehari, M. (2018). A conceptual framework for environmental risk and social vulnerability assessment in complex urban settings. *Urban Climate*. 26: 161–173. <https://doi.org/10.1016/j.uclim.2018.08.005>

McGrane, S. J. (2016). Impacts of urbanisation on hydrological and water quality dynamics, and urban water management: a review. *Hydrological Sciences Journal*. 61(13): 2295–2311. <https://doi.org/10.1080/02626667.2015.1128084>

Mrubata, K.; Nciizah, A. D.; Wakindiki, I. I. C.; Mudau, F. N. (2024). Effects of rainfall intensity and slope gradient on soil sealing and crusting, erosion, and phosphorus solubilizing bacteria. *Scientific African*. 23: eo2064. <https://doi.org/10.1016/j.sciaf.2024.eo2064>

Mukherjee, N.; Hugé, J.; Sutherland, W. J.; Mcneill, J.; Van Opstal, M.; Dahdouh-Guebas, F.; Koedam, N. (2015). The Delphi technique in ecology and biological conservation: Applications and guidelines. *Methods in Ecology and Evolution*. 6(9): 1097–1109. <https://doi.org/10.1111/2041-210X.12387>

O'Riordan, R.; Davies, J.; Stevens, C.; Quinton, J. N. (2021). The effects of sealing on urban soil carbon and nutrients. *SOIL*. 7(2): 661–675. <https://doi.org/10.5194/soil-7-661-2021>

Peroni, F.; Pristeri, G.; Codato, D.; Pappalardo, S. E.; De Marchi, M. (2020). Biotope area factor: An ecological urban index to geovisualize soil sealing in Padua, Italy. *Sustainability*. 12(1): 150. <https://doi.org/10.3390/SU12010150>

Pham, K. T.; Lin, T. H. (2023). Effects of urbanisation on ecosystem service values: A case study of Nha Trang, Vietnam. *Land Use Policy*. 128: 106599. <https://doi.org/10.1016/j.landusepol.2023.106599>

Piero, M.; Angelo, B.; Antonello, B.; Amedeo, D.; Carlo, D. M.; Michela, I.; Giuliano, L.; Florindo, M. A.; Paolo, P.; Simona, V.; Fabio, T. (2017). Soil sealing: Quantifying impacts on soil functions by a geospatial decision support system. *Land Degradation and Development*. 28(8): 2513–2526. <https://doi.org/10.1002/lrd.2802>

Pristeri, G.; Peroni, F.; Pappalardo, S. E.; Codato, D.; Castaldo, A. G.; Masi, A.; De Marchi, M. (2020). Mapping and assessing soil sealing in Padua municipality through biotope area factor index. *Sustainability*. 12(12): 5167. <https://doi.org/10.3390/su12125167>

Saaty, T. L. (2013). The modern science of multicriteria decision making and its practical applications: The AHP/ANP approach. *Operations Research*. 61(5): 1101–1118. <https://doi.org/10.1287/opre.2013.1197>

Seifollahi-Aghmiuni, S.; Kalantari, Z.; Egidi, G.; Gaburova, L.; Salvati, L. (2022). Urbanisation-driven land degradation and socioeconomic challenges in peri-urban areas: Insights from Southern Europe. *Ambio*. 51(6): 1446–1458. <https://doi.org/10.1007/s13280-022-01701-7>

Stevenson, A.; Zhang, Y.; Göçmen, Z. A.; Hartemink, A. E. (2025). Urbanization and sealing of fertile soils: A case study in Wisconsin 2001–2021. *Soil Security*. 19: 100183. <https://doi.org/10.1016/j.soisec.2025.100183>

Taherdoost, H. (2023). Analysis of simple additive weighting method (SAW) as a multiattribute decision-making technique: A step-by-step guide. *Journal of Management Science & Engineering Research*. 6(1): 21–24. <https://doi.org/10.30564/jmser.v6i1.5400>

Terán-Gómez, V. F.; Buitrago-Ramírez, A. M.; Echeverri-Sánchez, A. F.; Figueroa-Casas, A.; Benavides-Bolaños, J. A. (2025). Integrating AHP and GIS for Sustainable surface water planning: identifying vulnerability to agricultural diffuse pollution in the Guachal River watershed. *Sustainability*. 17(9): 4130. <https://doi.org/10.3390/su17094130>

Thomas, I. A.; Jordan, P.; Mellander, P. E.; Fenton, O.; Shine, O.; Ó hUallacháin, D.; Creamer, R.; McDonald, N. T.; Dunlop, P.; Murphy, P. N. C. (2016). Improving the identification of hydrologically sensitive areas using LiDAR DEMs for the delineation and mitigation of critical source areas of diffuse pollution. *Science of the Total Environment*. 556: 276–290. <https://doi.org/10.1016/j.scitotenv.2016.02.183>

Tóth, G.; Ivits, E.; Prokop, G.; Gregor, M.; Esteve, J. F.; Agràs, R. M.; Mancosu, E. (2022). Impact of soil sealing on soil carbon sequestration, water storage potentials and biomass productivity in functional urban areas of the European Union and the United Kingdom. *Land*. 11(6): 840. <https://doi.org/10.3390/land11060840>

Vieillard, C.; Vidal-Beaudet, L.; Dagois, R.; Lothode, M.; Vadepied, F.; Gontier, M.; Schwartz, C.; Ouvrard, S. (2024). Impacts of soil de-sealing practices on urban land-uses, soil functions and ecosystem services in French cities. *Geoderma Regional*. 38: e00854. <https://doi.org/10.1016/j.geodrs.2024.e00854>

Wei, Z.; Wu, S.; Yan, X.; Zhou, S. (2014). Density and stability of soil organic carbon beneath impervious surfaces in Urban Areas. *PLOS ONE*. 9(10): e109380. <https://doi.org/10.1371/journal.pone.0109380>

Xiao, R.; Su, S.; Zhang, Z.; Qi, J.; Jiang, D.; Wu, J. (2013). Dynamics of soil sealing and soil landscape patterns under rapid urbanization. *Catena*. 109: 1–12. <https://doi.org/10.1016/j.catena.2013.05.004>

Yu, W.; Hu, Y.; Cui, B.; Chen, Y.; Wang, X. (2019). The Effects of Pavement Types on Soil Bacterial Communities across Different Depths. *International Journal of Environmental Research and Public Health*. 16(10): 1805 <https://doi.org/10.3390/ijerph16101805>

Zambon, I.; Benedetti, A.; Ferrara, C.; Salvati, L. (2018). Soil Matters? A Multivariate Analysis of Socioeconomic Constraints to Urban Expansion in Mediterranean Europe. *Ecological Economics*. 146: 173–183. <https://doi.org/10.1016/j.ecolecon.2017.10.015>

Ziem Bonye, S.; Yenglier Yiridomoh, G.; Derbile, E. K. (2021). 'Urban expansion and agricultural land use change in Ghana: Implications for peri-urban farmer household food security in Wa Municipality.' *International Journal of Urban Sustainable Development*. 13(2): 383–399. <https://doi.org/10.1080/19463138.2021.1915790>